Simulations of Solvation Dynamics Using a Nonlinear Response Approach

P. van der Meulen, A. M. Jonkman, and M. Glasbeek*

Laboratory for Physical Chemistry, University of Amsterdam, Nieuwe Achtergracht 127, 1018 WS Amsterdam, The Netherlands

Received: June 25, 1997; In Final Form: November 3, 1997

Simulations of the time evolution of the probability distribution function of the solvation coordinate of a solute in liquid solution are presented. Assuming impulsive excitation of the ground-state population to the excited-state free energy surface, the time dependence of the probability distribution function of the solvation coordinate is obtained by solving the Smoluchowski diffusion equation. Emphasis is on the influence of anharmonicity in the expression for the free energy surfaces on the solvation dynamics and its implications for time-resolved fluorescence measurements.

1. Introduction

Solvation dynamics in polar liquids has received great interest in the past decade [for reviews, see ref 1]. The time-dependent response of the solvent upon photoinduced changes of the charge distribution within the solute molecules has been the main focus. An example of a molecule for which several solvation relaxation studies have been performed in recent years is the laser dye molecule DCM (4-(dicyanomethylene)-2-methyl-6-(*p*-(dimethylamino)styryl)-4*H*-pyran).[2−8] In polar solvents, DCM is known to exhibit an appreciable total Stokes shift (e.g., $\lambda_{abs} = 465$ nm and $\lambda_{fl} = 630$ nm in methanol[9]). The large Stokes shift arises mainly from the large difference (∼20 D) between the dipole moments of the molecule in its ground and the emissive excited charge transfer (CT) state.[9] Recently, we reported on femtosecond fluorescence up-conversion studies of the solvation dynamics for DCM.[3,7] In several polar solvents, DCM showed bimodal solvation behavior. A fast decay component (∼100 fs) was observed and attributed to the effect of inertial "free streaming" motions of the solvent molecules. The slower decay components, on a picosecond time scale, were considered to be representative of the contribution of diffusional reorientation motions to the solvation dynamics of the solute. Concomitant with the dynamic Stokes shift, a rapid initial increase (on a subpicosecond time scale) in the integrated emission intensity and an overall narrowing of the emission band could be discerned. It was conjectured that the excited-state electron transfer is preferentially to a higher lying, but nonemissive, charge transfer state which subsequently relaxes by internal conversion to the emissive charge transfer state. Starting from a modified Smoluchowski diffusion equation[1,10,11] and assuming free energy curves that show a parabolic dependence on the solvation coordinate, a model calculation of the population redistribution in the excited CT state following the excitation pulse was attempted. The approach yielded satisfactory results for the dynamic Stokes shift and the temporal behavior of the integrated emission intensity. However, the predicted time-dependence of the emission band shape parameters (bandwidth and height) showed a significant disparity with the experimental results.[7]

Emission band narrowing has been observed in previous solvation dynamics studies reported elsewhere.[4,12,13] Several processes have been considered to account for the narrowing phenomenon. One of these is vibrational cooling which equilibrates the vibrationally hot molecule (formed in the intramolecular vibrational relaxation (IVR) process[14−16] following the optical excitation pulse) with the bath.[4,14,16−19] Vibrational cooling is likely to occur on a picosecond time scale.[16−19] Alternatively, it has been proposed that spectral narrowing results from the dynamic solvation process itself.[12,13,20,21] In particular, narrowing may occur when the curvature of the free energy surface for the solute system in the excited state (as a function of the solvation coordinate) is larger than for the free energy surface for the system in the ground state.[20−28] A change in the curvature of the free energy might occur when the solute in its excited state dielectrically saturates the first solvation shell.[29−31] It is the purpose of this paper to explore solvation-induced band narrowing based on this latter mechanism in more detail by extending our previous simulations.[7] It will be shown that better agreement with the experimental data for DCM in polar solution can be obtained by including anharmonic terms in the expressions for the free energy curves as a function of the solvation coordinate. The results are a typical manifestation of nonlinear response in solvation dynamics. Nonlinear effects in ionic and dipolar solvation have been extensively investigated. Kakitani, Mataga, and Yoshimori[32−38] discussed the effects of dielectric saturation on the activation barrier and the reaction rate of the charge transfer in liquid solution. However, in a series of papers Tachiya has commented on several aspects of their work.[39−42] In more recent work, Yoshimori elaborated on the effects of nonlinear response on the dynamics of the solvation process using a generalized Smoluchowski−Vlasov equation.[43,44] Also, nonlinear effects have been included in molecular dynamics simulations of solvation dynamics.[45] In general, it has been concluded that nonlinear behavior is most pronounced when the solute is dissolved in protic solvents which may give rise to the formation of hydrogen bridges.[45−47] In this paper we focus on the solvation dynamics of the probe molecule DCM dissolved in ethylene glycol. From the combination of the large dipole moment of DCM in its excited state (∼26 D), i.e., much larger than the dipole moment of the coumarin solvation probes,[14,45] and the tendency of ethylene glycol toward hydrogen bonding, a marked nonlinear response may be expected for the system.

S1089-5639(97)02073-2 CCC: $15.00
Published on Web 02/20/1998

In the following section, we first briefly review the applied simulation method. Subsequently, a few typical results of the simulations for charge separation and recombination reactions are presented. Finally, the significance of the simulations for the specific case of DCM in ethylene glycol is discussed.

2. Method

We consider the free energy of the system in the ground state and in the excited state, $F^g(x)$ and $F^e(x)$, respectively, as a function of a generalized solvation coordinate, x, as follows[25−33]

$$F^g(x) = ax^4 + bx^2 \tag{1}$$

$$F^e(x) = ax^4 + bx^2 - x + \epsilon \tag{2}$$

where x has the dimension of energy, a and b are coefficients in the anharmonic and harmonic terms, respectively, and ϵ is the electronic energy difference between both states. The free energy gap is defined as $F^e(x_0^e) - F^g(x_0^g) = \Delta F^s + \epsilon$, where ΔF^s is the solvation free energy. Furthermore, the anharmonicity parameter is defined as

$$\beta = k_g/(k_e - k_g) \tag{3}$$

where

$$k_g = \partial^2 F^g(x)/\partial x^2|_{x=x_0^g} = 2b \tag{4}$$

and

$$k_e = \partial^2 F^e(x)/\partial x^2|_{x=x_0^e} = 12a(x_0^e)^2 + 2b \tag{5}$$

where x_0^g and x_0^e are the values of x corresponding to the minima in $F^g(x)$ and $F^e(x)$, respectively, and x_0^g equals zero. In terms of the solvation energy (ΔF^s) and the anharmonicity parameter (β), one obtains

$$a = -27(2\beta + 1)^3/[256(3\beta + 1)^4(\Delta F^s)^3] \tag{6}$$

$$b = -9\beta(2\beta + 1)/[8(3\beta + 1)^2\Delta F^s] \tag{7}$$

It follows that ΔF^s and β fully determine the functional behavior of the free energy curves $F^g(x)$ and $F^e(x)$. In section 3, the influence of anharmonicity on the solvation dynamics is examined numerically by considering the solvation dynamics for various combinations of the parameter values for ΔF^s and β. To be able to compare the various results, the simulations have been performed under the constraint that the Stokes shift of the system remains fixed. The Stokes shift is given by x_0^e (see Figure 1). Furthermore, from eqs 3−7, it follows that $x_0^e = (b/6a\beta)^{1/2}$. Thus, for a particular choice of ΔF^s and β, one can calculate a and b (cf. eqs 6 and 7) and also x_0^e. In the simulations of section 3, x_0^e was held fixed at 3000 cm^{-1}, which represents a typical value of the Stokes shift of a polar dye molecule in liquid polar solution. In Figure 1, we present a few characteristic free energy curves for $F^g(x)$ and $F^e(x)$ for $\beta = \pm\infty$, −2.00, and 0.10.

Upon impulsive photoexcitation of the solute molecules, the probability distribution of the solvation coordinate for the system in the ground state in thermal equilibrium, $\rho_g(x,0)$, is transferred nonadiabatically to the excited state (vertical excitation in Figure 1 from $F^g(x)$), resulting in a nonthermal equilibrium probability distribution, $\rho_e(x,0)$, for the system in the excited state.

The evolution of $\rho_e(x,t)$ with time t, as caused by the reorientational motions of the solvent molecules, was computed

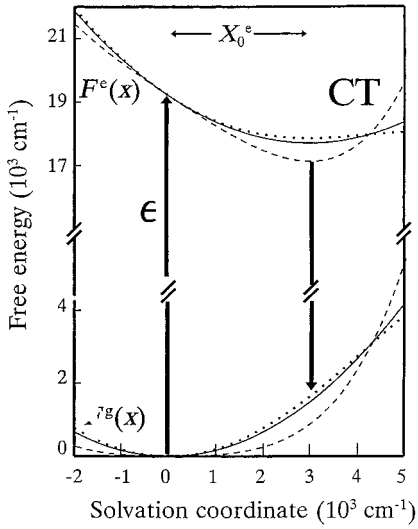

Figure 1. Free energy curves for the ground (neutral) and the excited (charge transfer) states for $\beta = \pm\infty$ (drawn curves), $\beta = -2.00$ (dotted curves), and $\beta = 0.10$ (dashed curves). In all cases the Stokes shift equals 3000 cm^{-1} . The energy gap between the neutral and the CT state was taken to be 19 200 cm^{-1}, which is the value used in the simulations of the experimental data of DCM in ethylene glycol (see text).

starting from the generalized Smoluchowski equation (GSE).[1,10,11] The GSE, which determines the diffusion of $\rho_e(x,t)$, has the form

$$\frac{\partial \rho_e(x,t)}{\partial t} = D_e(t)\frac{\partial}{\partial x}\left[\frac{\partial}{\partial x} + \frac{1}{k_B T}\frac{dF^e(x)}{dx}\right]\rho_e(x,t) \tag{8}$$

where $D_e(t)$ is the time-dependent solvation polarization diffusion coefficient given by

$$D_e(t) = -\langle(\delta x)^2\rangle\frac{\dot{S}_\nu(t)}{S_\nu(t)} \tag{9}$$

where k_B is the Boltzmann constant and T is the absolute temperature. As seen from eq 9, the time dependence of the solvation polarization diffusion coefficient, $D_e(t)$, is related to that of the normalized solvation coordinate time correlation function, $S_\nu(t)$. It is noted that eq 8, with a time-dependent diffusion coefficient $D_e(t)$, has been derived rigorously in the limit of a harmonic free energy surface.[48,49] On the other hand, when $S_\nu(t)$ is represented by a single exponential, $S_\nu(t) \sim \exp(-t\tau)$, $D_e(t)$ becomes independent of time,

$$D_e = (1/\tau)\langle(\delta x)^2\rangle \tag{10}$$

and eq 8 represents the well-known Fokker−Planck equation which is valid for any potential $F^e(x)$. Comparison with results from more accurate, but computationally more involved, simulations using the generalized Langevin equation[50−53] has shown that even for surfaces much more anharmonic than the ones considered in this paper, the Smoluchowski equation as in eq 8 gives satisfactory and physically meaningful results.[1,10,11] Likewise, we will henceforth apply eq 8, despite the fact that due to the anharmonicity in the free energy functions of interest in this paper, this equation cannot be derived rigorously.

In linear response, the time dependence of $S_\nu(t)$ equals that for the normalized dynamic fluorescence Stokes shift, $C(t)$,

$$C(t) = \frac{\nu^{fl_{max}}(t) - \nu^{fl_{max}}(\infty)}{\nu^{fl_{max}}(0) - \nu^{fl_{max}}(\infty)} \tag{11}$$

where $\nu^{fl}_{max}(t)$ represents the time-dependent frequency of the maximum of the fluorescence band.[54,55] Henceforth in this paper, it is considered that the temporal behavior of $D_e(t)$ will not be too different from that expected according to linear response theory, i.e., $D_e(t) \sim (dC(t)/dt)/C(t)$. The rationale behind this is that the anharmonic terms in $F^e(x)$ affect the width of $\rho_e(x,t)$, i.e., its diffusion with time, to a larger extent than the shift of the maximum of $\rho_e(x,t)$ with time. Thus, to simulate the time evolution of the shift in the case that anharmonicity is involved, it seems reasonable to adopt the approach for $D_e(t)$ as in the harmonic case. The time dependence of $C(t)$, in the case of DCM dissolved in a few polar solvents, has been experimentally determined recently from fluorescent up-conversion[5,6] and transient absorption experiments.[3,4,9] Thus, by making use of the experimental data for the dynamic and static Stokes shifts, it is possible to simulate $\rho_e(x,t)$ as a function of time for each pair of preselected values of β and ΔF^s.

As a last step, the time-dependent fluorescence spectrum is calculated using

$$I_{fl}(\nu,t) \propto \int dx\, g(\nu_0(x),\nu-\nu_0(x))\, \rho_e(x,t)\nu^3 \qquad (12)$$

where ν is the emission frequency, $g(\nu_0(x), \nu - \nu_0(x))$ is a line shape function characteristic of the Franck−Condon factor, and $\nu_0(x)$ is the solvation coordinate dependent energy gap between the excited state and the molecular ground state. We note that the distribution $\rho_e(x,t)$ in fact gives rise to inhomogeneous line broadening of the optical transition. Equation 12 shows that the simulated spectrum is obtained as the convolution of the homogeneously broadened component represented by the spectral function, $g(\nu(x))$, with an inhomogeneous broadening contribution given by $\rho_e(x,t)$.

3. Results and Discussion

We have performed simulations of $\rho_e(x,t)$ following the steps outlined above for a charge separation process and a charge recombination process. Figure 1 shows, as an illustrative example, the situation for a solute which can be photoexcited into a charge transfer (CT) state. Thus, in this example, charge separation is accomplished by the photoexcitation process and charge recombination is effectuated by emission. In addition, we report on results that simulate the temporal spectral behavior of DCM dissolved in ethylene glycol.

Figure 1 represents a few free energy curves for several values of β used in the simulations. Curves for positive and negative values of β are included. For $\beta > 0$, the curvature of the curve of the CT state at its equilibrium minimum is larger than that of the free energy of the system in the ground-state minimum, while for $\beta < -1$ the opposite holds. For $\beta \rightarrow \pm\infty$, the curvatures at the two minima are identical. Furthermore, in the latter cases the ground-state and CT state curves are parabolic and solvation behavior is linear. Maximum deviation from linear behavior is expected when β approaches the values -1 (from below) or 0 (from above). Note also that β cannot adopt values between -1 and 0. Intuitively we expect $\beta > 0$ because, in the presence of a large solute dipole moment, the fluctuations of the solvent will be reduced and, therefore, the force constant of the curve near its minimum to be larger.[20,21] Several molecular dynamics calculations have indicated that $\beta < 0$ is also possible;[26,45−47] most simulations tend to favor $\beta > 0$ for the CT state, however.[21−28,45−47]

The time dependence of $\rho_e(x,t)$ was solved from eq 8 for the case of a charge separation process (absorption in Figure 1) for the following parameter values. The Stokes shift was fixed at 3000 cm^{-1}, $T = 295$ K, and the time dependence of the diffusion coefficient was determined from eq 9, assuming a single-exponential decay for $S_\nu(t) \sim C(t) = \exp(-t/\tau)$, with a time constant of $\tau = 1$ ps. Since, upon photoexcitation at $t = 0$, it is assumed that the initial population of the ground state is impulsively transferred to the CT free energy surface, we have $\rho_e(x,0) \propto \exp(-F^g(x)/k_BT)$. As outlined above, the simulations were performed for different values of β. Table 1 collects the solvation energies for the different values for β which were used in the simulations. With these parameters, the time evolution of the population distribution as a function of x for the system in the excited state was computed for $0 < t < 7$ ps.

TABLE 1: Values of β Used in the Simulations with the Related Solvation Energies ΔF^s

β	ΔF^s (cm^{-1})[a]	β	ΔF^s (cm^{-1})[a]
10.0	−1524	0.2	−1969
5.0	−1547	−3.0	−1406
2.0	−1607	−5.0	−1446
1.0	−1687	−10.0	−1474
0.5	−1800	∞	−1500

[a] All values of ΔF^s are calculated for a fixed Stokes shift of 3000 cm^{-1}.

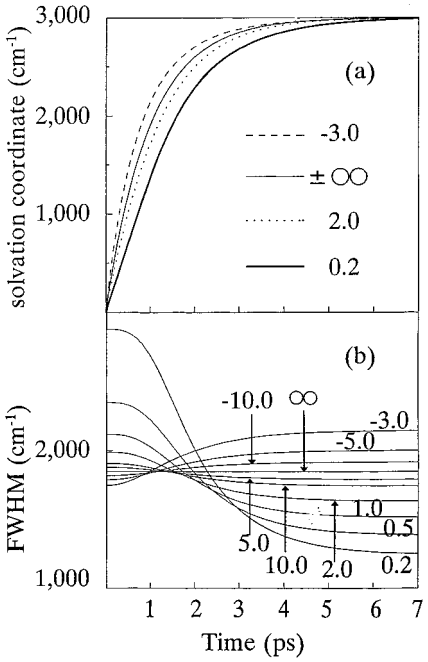

Figure 2. Time evolution of (a) the coordinate position of the population distribution maximum, x_{max}, and (b) the fwhm of the population distribution for a charge separation process with a fixed Stokes shift of 3000 cm^{-1} and the β values as indicated. The decay time of the solvent response function (see text) was taken to be 1 ps.

Results of the simulations for the charge separation reaction for a few values for β are presented in Figure 2. In Figure 2a we show how x_{max}, which is the value of x corresponding to the maximum in the function $\rho_e(x)$, shifts with time t as the solvation progresses. As expected for a diffusion type solvation relaxation process, in addition to a shift in x_{max}, which corresponds to the dynamic Stokes shift, the population distribution may spread out (or shrink) depending on β. This is illustrated in Figure 2b which shows how the full width at half-maximum (fwhm) of the function $\rho_e(x)$ changes with time when considered for different values of β.

As follows from Figure 2a, for the chosen set of parameter values, solvation relaxation is complete (i.e., the solvation coordinate change has become 3000 cm^{-1}) after about 7 ps,

irrespective of the value of β. However, the magnitude of β does affect the rate of the solvation process somewhat. For $\beta = -3.0$, the solvation is initially fastest, whereas the slowest initial solvation is obtained for relatively small positive values of β. For $\beta = \pm\infty$, i.e., the free energy curves of the ground and excited states are parabolic, the solvation rate is between that for the anharmonic cases with β being either positive ($\beta = 0.2$) or negative ($\beta = -3.0$).

To qualitatively discuss this variation of the solvation dynamics with β, we start by considering the time dependence of first moment $\langle x \rangle$, which is obtained directly from eq 8 and is given by

$$\frac{\partial}{\partial t}\langle x(t)\rangle = -\frac{D_e}{k_B T}\left\langle \frac{\partial F^e(x)}{\partial x}\right\rangle \tag{13}$$

Although in this paper, following most experimental studies that address the shift of the maximum of the fluorescence band, we emphasize the change in the position of the maximum of the probability distribution with time, the behavior of the mean of the population distribution, as expressed by eq 13, is expected to be similar and somewhat easier to calculate. Since $\partial F^e/\partial x = \partial F^g/\partial x - 1$, eq 13 can be rewritten as

$$\frac{\partial}{\partial t}\langle x(t)\rangle = -\frac{D_e}{k_B T}\left\langle \frac{\partial F^g(x)}{\partial x} - 1\right\rangle = -\frac{D_e}{k_B T}\left(\int_{-\infty}^{+\infty} \rho(x,t)\frac{\partial F^g(x)}{\partial x}\,dx - 1\right) \tag{14}$$

The integral in eq 14 can be written as a function of the potential energy surface $F^g(x)$ and the moments $M_i(t)$ of the probability distribution $\rho(x,t)$:

$$\int_{-\infty}^{+\infty} \rho(x,t)\left(\frac{\partial F^g(x)}{\partial x}\right) dx = 4aM_3 + 2bM_1 \tag{15}$$

Equation 15 illustrates that the dependence of the solvation rate on β as well as on time is not immediately transparent, since it depends on the moments of the probability distribution function up to third order. At time $t = 0$, it is easily verified that the solvation rate, $\partial\langle x\rangle/\partial t$ equals $+D_e/k_B T$ for all values of β, but immediately thereafter the solvation rates start to differ, as seen in Figure 2a.

To gain more insight, we turn to eq 8. The first term on the right-hand side of eq 8 gives rise to a spreading out (shrinking) of the probability distribution function only, but not to a shift of x_{max}. The second term, however, is relevant because it not only depends on $\partial F^e/\partial x$ (which, as already noted, in the limit of small values for x is not very different for the various values of β of Figure 1), but it contains also the factor $(\partial\rho_e(x,t)/\partial x)$. For the initial distribution, $\rho_e(x,0)$, one has that $(\partial\rho_e(x,t)/\partial x)$ is positive when $x < 0$ and negative when $x > 0$. Since $\partial F^e/\partial x < 0$ for $x \approx 0$, one has also that $(\partial F^e/\partial x)(\partial\rho_e(x,t)/\partial x)$ is negative when $x < 0$ and positive when $x > 0$. Thus, $\rho_e(x,0)$ will, as time progresses, decrease at the side where it rises (i.e., when $x < 0$), whereas $\rho_e(x,0)$ will increase for $x > 0$. In this way the shift of x_{max} with time is visualized. Obviously, when $|\partial\rho_e(x,t)/\partial x|$ becomes smaller, the rate, $\partial\rho_e(x,t)/\partial t$, becomes less as well. This is of relevance in considering the variation of the Stokes shift dynamics with β: when $\beta > 0$, the distribution $\rho_e(x,0)$ is relatively broad as compared to the case for $\beta < 0$, and thus $|\partial\rho_e(x,t)/\partial x|$ becomes relatively small. This is basically why the *initial* solvation rate for $\beta > 0$ is less than in the case when $\beta < 0$ (cf. Figure 2a). The conclusion is, therefore, that the variation in the initial solvation rates as a function β is not so much determined by the slope or curvature of $F^e(x)$ at small values for x, but rather by the width of the initial distribution of $\rho_e(x,0)$. This dependence on the initial width, which depends strongly on $\partial F^g(x)/\partial x$, is, of course, contained in eqs 14 and 15, but in a somewhat hidden fashion. In the final stage of the solvation process, for x near x_e, the influence of the other factors mentioned above, i.e., the slope and curvature, becomes more pronounced, and thus the solvation becomes fastest when relaxation is considered for the $F^e(x)$ curve with the steepest slope (when $\beta = 0.2$). Note that also in this case the fastest solvation ($\beta = 0.2$) corresponds to the probability distribution with the smallest width.

The time evolution of the fwhm of $\rho_e(x,t)$ is shown in Figure 2b for various values of β. For $\beta = -3.0$, the distribution $\rho_e(x,t)$ is seen to broaden. This is easily understood since, for $\beta = -3.0$, one has that $k_g > k_e$ and the probability distribution for $\rho_e(x,0)$, as determined by the Boltzmann factor $\exp(-F^g(x)/k_B T)$, will be narrow as compared to $\rho_e(x,\infty)$, the latter being representative of the probability distribution for x when the system has equilibrated in the excited state by solvation. Thus, as solvation proceeds, $\rho_e(x,t)$ will spread out and emission band broadening will occur. When $\beta = 0.2$, one has that $k_g < k_e$ and, in this case, $\rho_e(x,0)$ will be broader than eventually for the system in the equilibrated excited state; i.e., a narrowing of the emission bandwidth is expected, as indeed simulated in Figure 2b for a series of positive values for β.

As is clear from Figure 2b, for $\beta = \pm\infty$, i.e., when the free energy curves $F^e(x)$ and $F^g(x)$ are parabolic, the fwhm of $\rho_e(x,t)$ remains constant during the solvation process. Obviously, changes in the fwhm arise from nonlinear effects in the solvation dynamics. In this respect, our simulations seem to support the conjecture by Carter and Hynes[20,21] that any evolution in the fwhm of $\rho_e(x,t)$ represents a typical manifestation of nonlinear effects in solvation dynamics. It is interesting to note from a comparison of parts a and b of Figure 2 that the time scale of the change in the fwhm is the same as for the dynamic Stokes shift. Furthermore, the onset of the dynamic change in the fwhm of $\rho_e(x,t)$ seems somewhat retarded as compared to that of the dynamic Stokes shift. Only after the maximum has moved away from $x = x_0^g$ (=0), does the distribution begin to narrow (broaden). Initially, the contribution of the diffusive $(\partial^2 F^e/\partial x^2)$ term in eq 8, which is responsible for the narrowing (broadening), is not large enough. This is readily understood since $(\partial^2 F^e/\partial x^2) = 12ax^2 + 2b$(cf. eq 2), and thus, for small values of x, the influence of the anharmonicity term (which is responsible for the dynamic narrowing (broadening)) is still negligible.

In Figure 3, similar simulation results are shown for the case of a charge recombination reaction (emission in Figure 1), using the same parameter values as before. Note that now the dynamics occurs on the ground-state surface. Figure 3a shows the dynamic shift of the maximum of the ground-state population distribution, and Figure 3b is representative of the time-dependent change in the fwhm of $\rho_g(x,t)$. Again, the initial population distribution of $\rho_g(x,t)$ and the anharmonicity terms are pertinent to the solvation dynamics, albeit, as expected, the results obtained for the charge recombination reaction are opposite to those of the charge separation process. We now find that for $\beta = 0.2$ the solvation is initially faster than for $\beta = -3.0$. Taking into account the almost equal slopes of the ground-state free energy surfaces for the various values of β when $x \approx x_0^e \approx 3000$ cm^{-1}, this observation can be explained using the same reasoning as above. When $\beta = 0.2$, one has that the population distribution at $t = 0$, given by the Boltzmann

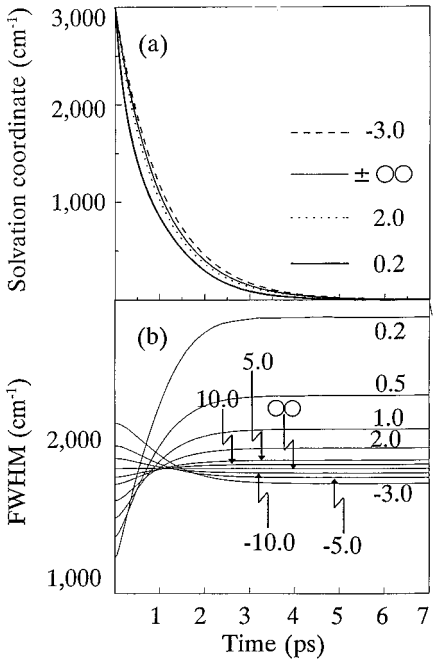

Figure 3. Time evolution of (a) the maximum of the population distribution and (b) the fwhm of the population distribution for a charge recombination process with a fixed Stokes shift of 3000 cm^{-1} and the β values as indicated. The decay time of the solvent response function (see text) was taken to be 1 ps.

factor $\exp(-F^e(x)/k_BT)$, is narrower, and therefore $|\partial\rho_g(x,0)/\partial x|$ is larger as compared to the cases where $\beta = -3.0$ or $\beta \rightarrow \pm\infty$. This leads one to expect that initial solvation is fastest for $\beta = 0.2$, in agreement with the simulation results. Eventually, however, the slopes of the $\beta = -3.0$ or $\beta \rightarrow \pm\infty$ free energy surfaces will become steeper, and thus, for these values of β, the solvation will be faster when x approaches zero.

The time dependence of the emission bandwidth has also been computed (cf. Figure 3b). As before, the sign of β determines whether a band broadening or narrowing will occur. If, for instance, $\beta > 0$, then the initial probability distribution of $\rho_g(x,0)$ will be narrower than the final distribution function $\rho_g(x,\infty)$, and this obviously results in a dynamic band broadening effect. Since the curvatures of the $F^g(x)$ curves when $x \approx x_0^e$ now show a significant variation with x (see, e.g., Figure 1), there is no retarded broadening effect in the charge recombination reaction, in contrast with the charge separation reaction.

Using the aforementioned approach, we have also attempted to simulate the experimentally determined spectral characteristics for DCM dissolved in ethylene glycol.[7] The following parameter values were used to solve $\rho_e(x,t)$ and $I_{fl}(\nu,t)$ from eqs 8 and 12, at $T = 295$ K. The solvent contribution to the Stokes shift was taken to be equal to the experimental value of 3000 cm^{-1}, and taking $\beta = 0.1$ one has that $\Delta F^s = -2076$ cm^{-1}. Furthermore, for the time-dependent diffusion coefficient, $D_e(t)$, we used the best fit experimental time dependence, $\sum a_i \exp(-\tau_i/t)$, with $a_1 = 0.5$, $\tau_1 = 0.1$ ps, $a_2 = 0.3$, $\tau_2 = 1.5$ ps, and $a_3 = 0.2$, $\tau_3 = 30$ ps. As before, impulsive excitation was assumed. The excitation energy, ϵ, was taken to be 19 200 cm^{-1}. The line shape function, $g(\nu_0(x), \nu - \nu_0(x))$, characteristic of the Franck−Condon overlap was taken to be Gaussian, with a width (fwhm) of 1400 cm^{-1}. The calculated emission spectra $I_{fl}(\nu,t)$ for various values of t were fitted with a log-normal line shape function.[14] A few typical results are presented in Figure 4. Figure 4a shows the experimental (full dots) and computed (crosses) time dependences of the position of the band maximum. Figure 4b shows the time dependence of the emission

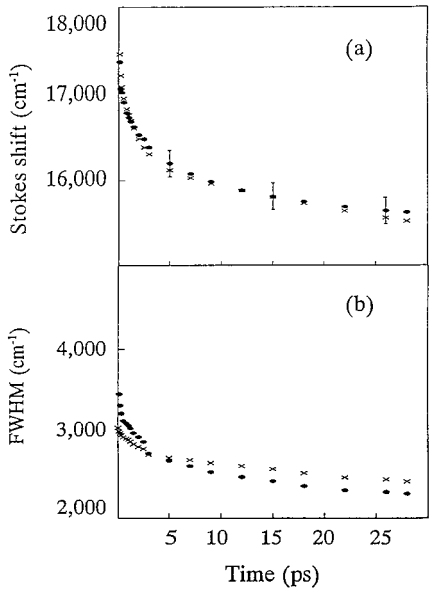

Figure 4. Experimental and simulated (a) dynamic Stokes shifts and (b) emission bandwidth (fwhm) for DCM dissolved in ethylene glycol: ●, experimental; ×, simulated.

bandwidth (fwhm). Upon comparison of the simulated dynamic Stokes shift with the experimental data in Figure 4a, it is clear that the model calculations performed for $\beta = 0.1$ indeed yield satisfactory results. With regard to the fwhm (cf. Figure 4b), the main experimental features can be reproduced; the agreement between simulation and experiment is to within about 10%.

In Figure 1, we have included the plot for the free energy curves for the system in the ground and excited states as computed for the aforementioned parameters. It is clear that these energy curves exhibit considerable anharmonicity characteristic of nonlinear response, with a larger curvature for the excited state than for the ground state ($\beta = 0.1$). It has been argued by means of Monte Carlo calculations that a ratio of $k_e/k_g \approx 11$ (i.e., $\beta = 0.1$) may indeed be expected in the event of dielectric saturation of the first solvent shell around the charged solute.[29−31] On the other hand, recently it has been discussed[21−28,37,38,45−47] that β values in the range between 0.5 and 2.0 seem more reasonable.

As is seen from Figure 4b, the simulated width (∼3000 cm^{-1}) of the *initial* DCM fluorescence band is slightly smaller than the value determined from the experimental data (∼3500 cm^{-1}). The deviation may not be significant considering the experimental error (10%) and the simplifications in the theoretical approach. However, vibrational relaxation may play a role here as well. It is conceivable that even when IVR is completed within 100 fs after the excitation of the DCM molecules,[14−16] the latter are still vibrationally hot and not yet in thermal equilibrium with the bath of solvent molecules. Subsequent vibrational cooling within a few picoseconds seems realistic.[16−19] Since the fluorescence spectrum of vibrationally hot DCM molecules will be broadened with respect to the continuous-wave (CW) emission band, as long as the vibrational cooling takes place, this may be accompanied by a further reduction of the emission bandwidth. Additionally, it is remarked that, in our simulations, the Franck−Condon overlap function was chosen to be a Gaussian shaped function with a line width that is independent of the generalized solvation coordinate, x. For the solvation of DCM in polar liquids, this may not be strictly valid. If, as the system relaxes, the Gaussian line shape function narrows, this narrowing could possibly account for the somewhat lower line width at longer times than actually simulated (cf.

Figure 4b). Finally, it has been recently proposed by Kovalenko et al.[8] that in DCM the excited-state charge transfer takes place on a time scale of about 100 fs. The same authors also suggested that the fluorescence from the locally excited state is much broader than the charge transfer state emission. The former would correspond to the steady-state emission observed in an apolar solvent (e.g., cyclohexane), while the latter resembles the ordinary fluorescence in a polar solvent (as e.g. methanol). As is apparent from Figure 4b, indeed we find experimentally that at very early times after the excitation ($t <$ 500 fs) the bandwidth as deduced in the spectral reconstruction procedure is significantly larger than simulated. Furthermore, Kovalenko et al.[8] report an increase in their measured gain on a time scale similar to that of the integrated fluorescence intensity increase previously observed by us.[3,7] Evidently, additional features, not included in the simulations, have to be considered when the electronic character of the fluorescent state is changing with time.

In an attempt to further elucidate the influence of intramolecular relaxation (IVR, vibrational cooling, internal conversion, etc.) on the time-resolved emission spectra, we have recently performed fluorescence up-conversion experiments for DCM in which the temporal evolution of the emission spectrum was measured as a function of the excitation energy.[56] After excitation of DCM into the vibration*less* photoexcited state, the solvation dynamics after 500 fs is found to be no different to that already previously reported by us.[7] Thus, using laser selective excitation, it is shown that, at least after 500 fs, the dynamic changes in the emission bandwidth are not due to any intramolecular relaxation process, in particular vibrational cooling.[16−19]

In summary, starting from a Smoluchowski diffusion equation, we have simulated dynamic Stokes shift as well as band narrowing (or, in some cases, broadening) effects following pulsed excitation of an optical transition. Emphasis has been on the effects that arise when anharmonicity in the free energy curves as a function of the solvation coordinate is taken into account explicitly. It has been shown that the anharmonicity causes a narrowing (broadening) of the optical transition band on the time scale of the solvation. The simulations can account for the observations previously reported for fluorescent DCM dissolved in ethylene glycol provided a pronounced anharmonicity of the free energy curves is assumed. A few additional factors relevant for the observed bandwidth changes have also been discussed.

Acknowledgment. This work was supported in part by The Netherlands Foundation for Chemical Research (SON) with financial aid from The Netherlands Organization for Scientific Research (NWO).

References and Notes

(1) Kosower, B. M.; Huppert, D. *Annu. Rev. Phys. Chem.* **1986**, *37*, 127. Simon, J. D. *Acc. Chem. Res*. **1988**, *21*, 128. Maroncelli, M.; MacIniis, J.; Fleming, G. R. *Science* **1989**, *243*, 1674. Bagchi, B. *Annu. Rev. Phys. Chem*. **1989**, *40*, 115. Barbara, P. F.; Jarzeba, W. *Adv. Photochem*. **1990**, *15*, 1. Hynes, J. T. *Nature* **1994**, *369*, 439. Rossky, P. J.; Simon, J. D. *Nature* **1994**, *370*, 263.

(2) Easter, D. C.; Baronavski, A. P. *Chem. Phys. Lett*. **1993**, *201*, 153.

(3) Zhang, H.; Jonkman, A. M.; van der Meulen, P.; Glasbeek, M. *Chem. Phys. Lett*. **1994**, *224*, 551.

(4) Gustavsson, T.; Baldacchino, G.; Mialocq, J. C.; Pommeret, S. *Chem. Phys. Lett*. **1995**, *236*, 587.

(5) Pommeret, S.; Gustavsson, T.; Naskrecki, R.; Baldacchino, G.; Mialocq, J. C. *J. Mol. Liq*. **1995**, *64*, 101.

(6) Martin, M.; Plaza, P.; Meyer, Y. H. *Chem. Phys*. **1995**, *192*, 367.

(7) van der Meulen, P.; Zhang, H.; Jonkman, A. M.; Glasbeek, M. *J. Phys. Chem*. **1996**, *100*, 5367.

(8) Kovalenko, S. A.; Ernsting, N. P.; Ruthmann, J. *Chem. Phys. Lett*. **1996**, *258*, 445.

(9) Meyer, M.; Mialocq, J. C. *Opt. Commun*. **1987,** *64*, 264.

(10) Tominaga, K.; Walker, G. C.; Jarzeba, W.; Barbara, P. F. *J. Phys. Chem*. **1991**, *95*, 10475.

(11) Tominaga, K.; Walker, G. C.; Kang, T. J.; Barbara, P. F.; Fonseca, T. *J. Phys. Chem*. **1991**, *95*, 10485.

(12) Maroncelli, M.; Fleming, G. R. *J. Chem. Phys*. **1988**, *89*, 5044.

(13) Su, S. G.; Simon, J. D. *Chem. Phys. Lett*. **1989**, *158*, 423.

(14) Horng, M. L.; Gardecki, J. A.; Papazyan, A.; Maroncelli, M. *J. Phys. Chem*. **1995,** *99*, 17311.

(15) Taylor, A. J.; Erskine, D. J.; Tang, C. L. *Chem. Phys. Lett*. **1984,** *103*, 430.

(16) Mokhtari, A.; Chebira, A.; Chesnoy, J. *J. Opt. Soc. Am. B* **1990**, *7*, 1551.

(17) Laermer, F.; Israel, W.; Elsaesser, T. *J. Opt. Soc. Am. B* **1990**, *7*, 1604.

(18) Elsaesser, T.; Kaiser, W. *Annu. Rev. Phys. Chem*. **1991,** *42*, 83.

(19) Laermer, F.; Elsaesser, T.; Kaiser, W. *Chem. Phys. Lett*. **1989**, *156*, 381.

(20) Carter, E. A.; Hynes, J. T. *J. Phys. Chem*. **1989**, *93*, 2184.

(21) Carter, E. A.; Hynes, J. T. *J. Chem. Phys*. **1991**, *94*, 5961.

(22) Calef, D. F.; Wolynes, P. G. *J. Chem. Phys*. **1983**, *78*, 470.

(23) King, G.; Warshel, A. *J. Chem. Phys*. **1990**, *93*, 8682.

(24) Maroncelli, M. *J. Chem. Phys*. **1991**, *94*, 2084.

(25) Papazyan, A.; Maroncelli, M. *J. Chem. Phys*. **1991,** *95*, 9219.

(26) Fonseca, T.; Ladanyi, B. M.; Hynes, J. T. *J. Phys. Chem*. **1992,** *96*, 4085.

(27) Georgievskii, Y. *J. Chem. Phys*. **1996,** *104*, 5251.

(28) Ichiye, T. *J. Chem. Phys*. **1996,** *104*, 7561.

(29) Kakitani, T.; Mataga, N. *Chem. Phys. Lett*. **1986,** *124*, 437.

(30) Hatano, Y.; Saito, M.; Kakitani, T.; Mataga, N. *J. Phys. Chem*. **1988**, *92*, 1008.

(31) Hatano, Y.; Kakitani, T.; Yoshimori, A.; Saito, M.; Mataga, N. *J. Phys. Soc. Jpn*. **1990,** *59*, 1104.

(32) Kakitani, T.; Mataga, N. *J. Phys. Chem*. **1987,** *91*, 6277.

(33) Yoshimori, A.; Kakitani, T.; Enomoto, Y.; Mataga, N. *J. Phys. Chem*. **1989**, *93*, 8316.

(34) Saito, M.; Kakitani, T. *Chem. Phys. Lett*. **1990,** *172*, 169.

(35) Enomoto, Y.; Kakitani, T.; Yoshimori, A.; Hatano, Y.; Saito, M. *Chem. Phys. Lett*. **1991**, *178*, 235.

(36) Enomoto, Y.; Kakitani, T.; Yoshimori, A.; Hatano, Y. *Chem. Phys. Lett*. **1991,** *186*, 366.

(37) Hatano, Y.; Kakitani, T.; Enomoto, Y.; Yoshimori, A. *Mol. Simul*. **1991**, *6*, 191.

(38) Yoshimori, A.; Kakitani, T. *J. Phys. Soc. Jpn*. **1992**, *61*, 2577.

(39) Tachiya, M. *Chem. Phys. Lett*. **1989**, *159*, 505.

(40) Tachiya, M. *J. Phys. Chem*. **1989**, *93*, 7050.

(41) Tachiya, M.; Murata, S. *J. Phys. Chem*. **1992**, *96*, 8441.

(42) Tachiya, M. *J. Phys. Chem*. **1993**, *97*, 5911.

(43) Yoshimori, A. *Chem. Phys. Lett*. **1991,** *184*, 76.

(44) Yoshimori, A. *J. Mol. Liq*. **1995,** *65/66*, 297.

(45) Kumar, P. V.; Maroncelli, M. *J. Chem. Phys*. **1995**, *103*, 3038 and references therein.

(46) Fonseca, T.; Ladanyi, B. M. *J. Phys. Chem*. **1991,** *95*, 2116.

(47) Fonseca, T.; Ladanyi, B. M. *J. Mol. Liq*. **1994,** *60*, 1.

(48) San Miguel, M.; Sancho, J. M. *J. Stat. Phys*. **1980,** *22*, 605.

(49) Okuyama, S.; Oxtoby, D. W. *J. Chem. Phys*. **1986**, *84*, 5824.

(50) Fonseca, T. *J. Chem. Phys*. **1989**, *91*, 2869.

(51) Fonseca, T.; Cunha, M. *Chem. Phys. Lett*. **1989,** *155*, 385.

(52) Fonseca, T. *Chem. Phys. Lett*. **1989,** *162*, 491.

(53) Kang, T. J.; Jarzeba, W.; Barbara, P. F.; Fonseca, T. *Chem. Phys*. **1990**, *149*, 81.

(54) Chandler, D. *Introduction to Modern Statistical Mechanics*; Oxford University Press: New York, 1987.

(55) Chandra, A.; Bagchi, B. *Chem. Phys. Lett*. **1990,** *165*, 93.

(56) Zhang, H.; van der Meer, M.; Glasbeek, M. Unpublished results.